

## Matrix-Isolation Studies of Alkali-Metal and Thallium Perrhenates. IR Spectrum of $^{18}\text{O}$ -Enriched $\text{TlReO}_4$ and Dimerization of the $\text{MReO}_4$ Species

L. BENCIVENNI,<sup>†</sup> H. M. NAGARATHNA, D. W. WILHITE, and K. A. GINGERICH\*

Received June 7, 1983

A previous infrared matrix-isolation study on  $\text{CsReO}_4$  and  $^{18}\text{O}$ -enriched  $\text{CsReO}_4$  has been extended to other alkali-metal and thallium perrhenates.  $^{18}\text{O}$ -substitution experiments have established for  $\text{TlReO}_4$  a  $C_{2v}$  bidentate structure. The distortion of the  $\text{ReO}_4^-$  anion from the  $T_d$  configuration occurs in the  $C_{2v}$  perrhenates,  $\text{MReO}_4$ . The metal isotopic shifts, the  $\nu_{B_2} - \nu_{B_1}$  splitting of the  $\nu_3(T_2)$  mode of the free anion, and the band intensity ratios are used to discuss the distortion. The distortion is small in the alkali perrhenates and larger in  $\text{TlReO}_4$ . The dimerization of the  $\text{MReO}_4$  species has been studied in  $\text{N}_2$  and Ar matrices, and for the dimers,  $\text{M}_2(\text{ReO}_4)_2$ , a bridged  $D_{2h}$  symmetry has been suggested.

### Introduction

Ionic vapor species of metal-coordinated oxyanions are now being reexamined because some of the recent electron diffraction studies<sup>1,2</sup> have led to serious doubts about the earlier proposed structures. High-temperature electron diffraction is used almost exclusively for determining the gas-phase geometries of low-volatility compounds, and matrix-isolation spectroscopy is a very useful supplement for these studies.

The coordination character of this class of compounds, usually termed ternary oxides, is similar in a wide range of molecules such as in the  $D_{2d}$   $\text{M}_2\text{SO}_4$ ,<sup>3</sup>  $C_{2v}$   $\text{MVO}_3$ ,<sup>4</sup> and  $\text{MAsO}_2$ , and  $\text{MSbO}_2$ ,<sup>5</sup> molecules.

The electron diffraction study by Spiridonov et al.<sup>6</sup> has established a monodentate structure for gaseous  $\text{KReO}_4$ , and this is at variance with newly available results. In fact we have very recently characterized, with the aid of  $^{18}\text{O}$ -substitution experiments, the IR spectra of matrix-isolated  $\text{CsReO}_4$  for which a bidentate structure of  $C_{2v}$  symmetry has been established.<sup>7</sup> An electron diffraction study on  $\text{CsReO}_4$ <sup>8</sup> is consistent with our findings, and the same conclusions drawn for  $\text{CsReO}_4$  might be extended to  $\text{KReO}_4$  as well as to the other alkali-metal perrhenates. Finally, we became aware of an electron diffraction study on  $\text{TlReO}_4$  by Ugarov et al.<sup>9</sup> that has been interpreted assuming a bidentate-ring model identical with that of  $\text{CsReO}_4$ . One might be able to confirm that gaseous  $\text{TlReO}_4$  is isostructural with  $\text{CsReO}_4$  from the analysis of its  $^{16}\text{O}/^{18}\text{O}$  IR isotopic pattern. The reinforcement of the intensity of some of the  $\text{TlRe}^{16}\text{O}_4$  vibrations due to possible overlaps with certain modes of the  $^{16}\text{O}/^{18}\text{O}$  mixed isotopomers would be in fact expected.

In the present investigation, a systematic IR study is carried out on all alkali and thallium perrhenates. We report the  $^{18}\text{O}$ -enrichment studies on  $\text{TlReO}_4$  to establish the structure. The distortion of the  $\text{ReO}_4^-$  anion from  $T_d$  configuration will be discussed in terms of the metal isotopic shifts, the  $\Delta\nu_3(T_2)$  splitting, and the band intensity ratios. Finally, the dimerization of  $\text{MReO}_4$  species will also be discussed.

### Experimental Section

The samples of  $\text{NaReO}_4$ ,  $\text{KReO}_4$ , and  $\text{CsReO}_4$  were commercially available from Alfa products.  $\text{LiReO}_4$ ,  $\text{RbReO}_4$ , and  $\text{TlReO}_4$  were prepared from the metal carbonates and  $\text{Re}_2\text{O}_7$  as starting materials. About 1 g of powdered rhenium was heated in a quartz tube in an oxygen atmosphere. The oxidation reaction occurred in two steps:  $\text{ReO}_3$  was initially obtained, and after prolonged heating, the reddish oxide turned to the green-yellow heptoxide  $\text{Re}_2\text{O}_7$ . The process took about 30 to 40 min. Subsequently the metal carbonates were neutralized with a solution of  $\text{Re}_2\text{O}_7$  and  $\text{H}_2\text{O}$ , yielding the corresponding perrhenates at the ultimate products. The same synthetic route was

followed to prepare isotopically pure and enriched samples of cesium and thallium perrhenates. Here, rhenium was oxidized with  $^{18}\text{O}_2$  gas (99%), and  $\text{Re}_2^{18}\text{O}_7$  was dissolved in  $\text{H}_2^{18}\text{O}$  (99% in  $^{18}\text{O}$ ). Some of the enriched samples were also obtained from an  $^{18}\text{O}$ -exchange reaction in  $\text{H}_2^{18}\text{O}$ . The solutions were left for several weeks in sealed Pyrex vials, and they were gently evaporated, crystallized, and outgassed under vacuum.

The studied perrhenates were vaporized from alumina crucibles at the following temperatures: lithium, sodium, and potassium perrhenates at ca. 850 K, rubidium perrhenate at ca. 770 K, cesium perrhenate at ca. 745 K, and thallium perrhenate at ca. 625 K. High-purity (99.9995%)  $\text{N}_2$  and Ar have been used as matrix gases.

The effusing vapors were collected with a large amount of matrix gas on a CsI window at 13 K. The alkali and thallium perrhenates were also studied in less dilute matrices and from depositions at 25 K.

Details of the matrix-isolation apparatus are reported elsewhere.<sup>3</sup> The IR spectra were recorded on a Perkin-Elmer 580-B spectrometer calibrated before each experiment vs. the bands at 969.9 and 1028.3  $\text{cm}^{-1}$  of a standard polystyrene film and vs. the bands of  $\text{CO}_2$  and  $\text{H}_2\text{O}$  vapor.

The instrument was continuously purged with dry air during the experiments. The highest achieved resolution was 0.3  $\text{cm}^{-1}$ , and the measured frequencies are accurate to within  $\pm 0.5 \text{ cm}^{-1}$ .

### IR Spectra of the Matrix-Isolated $\text{MReO}_4$ Perrhenates

The IR spectra of  $\text{LiReO}_4$ ,  $\text{NaReO}_4$ ,  $\text{KReO}_4$ ,  $\text{CsReO}_4$ ,  $\text{RbReO}_4$ , and  $\text{TlReO}_4$  have been measured in  $\text{N}_2$  and Ar matrices. The spectrum of  $\text{RbReO}_4$  is shown in Figure 1, and the experimental frequencies of all the studied perrhenates are reported in Table I. These perrhenates have IR patterns similar to that of  $\text{CsReO}_4$ ,<sup>7</sup> consisting of an intense triplet and a less prominent higher frequency band. Except for  $\text{LiReO}_4$  and  $\text{TlReO}_4$ , these molecules have frequencies only slightly different from those of  $\text{CsReO}_4$ . This fact clearly indicates that the stretching vibrations of the  $\text{ReO}_4^-$  oxyanion are virtually uncoupled from the interionic modes involving the metal cation the latter of which are expected to occur in the far IR.<sup>10,11</sup> These spectra also indicate that the alkali-metal

<sup>†</sup> Present address: Centro Termodinamica Chimica Alte Temperature (CNR), Dipartimento di Chimica, Università di Roma, 00185 Rome, Italy.

- (1) Yu. S. Ezhov, S. M. Tolmachev, and N. G. Rambidi, *Zh. Strukt. Khim.*, **13**, 910 (1972).
- (2) K. P. Petrov, V. A. Kulikov, V. V. Ugarov, and N. G. Rambidi, *Zh. Strukt. Khim.*, **21**, 71 (1980).
- (3) R. M. Atkins and K. A. Gingerich, *Chem. Phys. Lett.*, **53**, 347 (1978).
- (4) L. Bencivenni and K. A. Gingerich, *J. Mol. Struct.*, **96**, 197 (1983).
- (5) L. Bencivenni and K. A. Gingerich, *J. Mol. Struct.*, **99**, 23 (1983).
- (6) V. P. Spiridonov, A. N. Khodchenkov, and P. A. Akishin, *Vestn. Mosk. Univ., Ser. 2: Khim.*, **6**, 34 (1965).
- (7) L. Bencivenni, H. M. Nagarathna, and K. A. Gingerich, *Chem. Phys. Lett.*, **99**, 258 (1983).
- (8) K. P. Petrov, V. V. Ugarov, and N. G. Rambidi, *Zh. Strukt. Khim.*, **21**, 189 (1980).
- (9) N. M. Roddatis, S. M. Tolmachev, V. V. Ugarov, Yu. S. Ezhov, and N. G. Rambidi, *Zh. Strukt. Khim.*, **15**, 693 (1974).

Table I. IR Frequencies ( $\text{cm}^{-1}$ ) and Band Assignments of the Stretching Modes of the  $\text{ReO}_4^-$  Anion in  $C_{2v}$   $\text{MReO}_4$  Molecules

	$\text{N}_2$ matrix				Ar matrix			
	$A_1$	$B_2$	$A_1$	$B_1$	$A_1$	$B_1$	$A_1$	$B_1$
$\text{LiReO}_4$	955.7	945.6	939.8	849.9	977.4	956.7	901.0	869.2
$\text{NaReO}_4$	973.1	945.9	912.5	887.7	970.4	946.7	905.7	876.7
$\text{KReO}_4$	969.9	941.4	914.4	892.2	969.3	943.3	909.3	883.3
$\text{RbReO}_4$	969.9	941.1	914.6	893.3	968.2	941.1	906.4	881.3
$\text{CsReO}_4^a$	969.9	940.8	913.6	892.7	967.6	940.3	905.0	880.0
$\text{TlReO}_4$	976.1	953.0	895.4	860.1	976.0	954.6	883.0	842.8

<sup>a</sup>  $\text{N}_2$  matrix frequencies from ref 7.

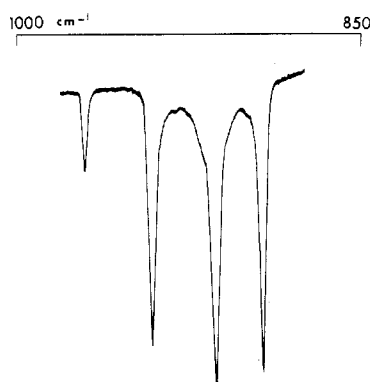


Figure 1. IR spectrum of  $\text{RbReO}_4$  isolated in  $\text{N}_2$  matrix.

perrhenates are likely to be isostructural with  $\text{CsReO}_4$  for which we have established a  $C_{2v}$  bidentate structure with the aid of  $^{18}\text{O}$  substitution. Therefore, the same vibrational assignment of the stretching are likely to be of the  $\text{ReO}_4^-$  anion in  $C_{2v}$   $\text{CsReO}_4$  can be extended to the other alkali perrhenates.

$^{18}\text{O}$  substitution in  $\text{CsReO}_4$  establishes that the highest frequency occurring at ca.  $970\text{ cm}^{-1}$  arises from the IR activation of the  $\nu_1(A_1)$  mode of the free  $\text{ReO}_4^-$  anion ( $T_d$  symmetry) and the bands of the prominent lower frequency triplet are the components of the splitting of the  $\nu_3(T_2)$  vibration. The normal-coordinate calculations performed on  $\text{CsReO}_4$  and its  $^{18}\text{O}$ -enriched isotopomers also provide the symmetry species of the components of the splitting. The  $\nu_3(T_2)$  mode splits in the  $C_{2v}$ -coordinated  $\text{ReO}_4^-$  oxyanion into the triplet ( $B_2 + A_1 + B_1$ ) for which  $\nu_{B_2} > \nu_{A_1} > \nu_{B_1}$ . It is interesting to regard this trend in a different context. The bidentate coordination of the  $\text{ReO}_4^-$  anion permits us to distinguish the rhenium-oxygen bonds between terminal or uncoordinated and bridged or coordinated bonds. The equivalence in the free  $\text{ReO}_4^-$  anion of the rhenium-oxygen bonds is lifted in the coordinated perrhenate group. Therefore, in the  $C_{2v}$   $\text{MReO}_4$  molecules the rhenium-oxygen terminal bond is expected to have a larger force constant than the bridged bond, thus suggesting a likely double-bond character for the uncoordinated  $\text{Re}=\text{O}$  bond. This has been tested by normal-coordinate calculations performed on the basis of the observed IR frequencies of  $\text{CsRe}^{16}\text{O}_4$ , of  $\text{CsRe}^{18}\text{O}_4$ , and of the  $^{18}\text{O}/^{16}\text{O}$  mixed species.<sup>7</sup>

In the alkali  $\text{MReO}_4$  molecules the stretching modes of the  $\text{ReO}_2$  terminal group ( $A_1 + B_2$ ) and of the  $\text{MO}_2\text{Re}$  frame ( $A_1 + B_1$ ) follow the order  $\nu(A_1) > \nu(B_2) > \nu(A_1) > \nu(B_1)$  in which the totally symmetric modes occur at higher frequencies than the antisymmetric vibrations  $B_2$  and  $B_1$ . Here the positions of the  $\nu(A_1)$ ,  $\nu(B_2)$ , and  $\nu(B_1)$  modes are reversed with respect

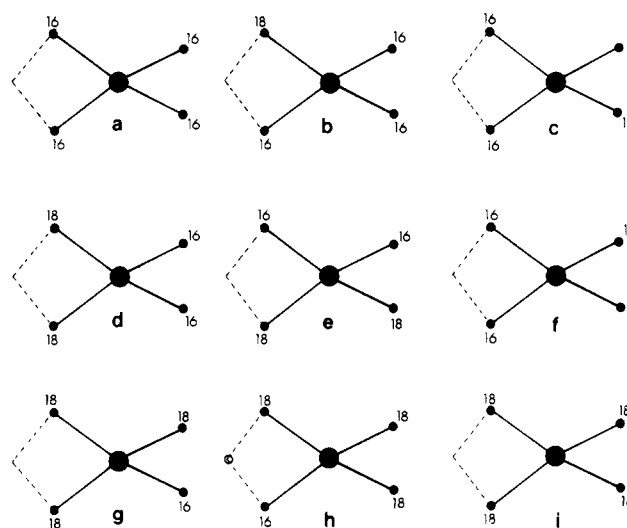


Figure 2. Isotopomers arising from random  $^{18}\text{O}$  substitution in  $C_{2v}$   $\text{TlReO}_4$ .

Table II.  $\text{ReO}_4^-$  Anion Stretching Vibrations in an  $^{18}\text{O}$ -Substituted  $\text{MReO}_4$  Molecule

isotopomers <sup>a</sup>	vibrational anal.
$\text{MRe}^{16}\text{O}_4$ (a) [1]	$C_{2v}$ ( $2A_1 + B_2 + B_1$ )
$\text{MRe}^{16}\text{O}_3^{18}\text{O}$ (b) [2]	$C_s$ ( $3A' + A''$ )
$\text{MRe}^{16}\text{O}_2^{18}\text{O}_2$ (c) [2]	$C_s$ ( $3A' + A''$ )
$\text{MRe}^{16}\text{O}_2^{18}\text{O}_2$ (d) [1]	$C_{2v}$ ( $2A_1 + B_2 + B_1$ )
$\text{MRe}^{16}\text{O}_2^{18}\text{O}_2$ (e) [4]	$C_1$ (4A)
$\text{MRe}^{16}\text{O}_2^{18}\text{O}_2$ (f) [1]	$C_{2v}$ ( $2A_1 + B_2 + B_1$ )
$\text{MRe}^{16}\text{O}^{18}\text{O}_3$ (g) [2]	$C_s$ ( $3A' + A''$ )
$\text{MRe}^{16}\text{O}^{18}\text{O}_3$ (h) [2]	$C_s$ ( $3A' + A''$ )
$\text{MRe}^{18}\text{O}_4$ (i) [1]	$C_{2v}$ ( $2A_1 + B_2 + B_1$ )

<sup>a</sup> The letters in parentheses refer to the isotopomers shown in Figure 2. The numbers in brackets are the statistical weights of the isotopomers.

to the isostructural perchlorates,  $\text{MClO}_4$ .<sup>12</sup> This fact is mainly due to the mass of the rhenium atom, which is heavier than the chlorine atom. The IR spectra of the  $\text{MReO}_4$  molecules isolated in  $\text{N}_2$  and Ar matrices do not show other bands in the low-frequency region in which the  $\text{ReO}_4^-$  deformations and the metal-cation modes might be expected. The  $\text{ReO}_4^-$  deformations fall in the range of the  $\nu_4(T_2)$  mode,<sup>13</sup> which in the  $C_{2v}$  perrhenates must appear as a triplet. Actually some of the matrix-isolated perrhenates show bands ranging between  $315$  and  $350\text{ cm}^{-1}$ . These feeble and somewhat vanishing absorptions could not be confidently assigned. The interionic modes in these ionic vapors lie in the far-IR region as has been occasionally observed in other species.<sup>10,11</sup> Attempts to measure these low-frequency bands gave no result because of their very low intensity.

Although the IR spectrum of  $\text{TlReO}_4$  might be interpreted assuming  $C_{2v}$  symmetry, it seems more appropriate to base any

(10) L. Bencivenni and K. A. Gingerich, *J. Mol. Struct.*, **98**, 195 (1983).

(11) H. M. Nagarathna, K. A. Gingerich, and L. Bencivenni, submitted for publication in *J. Chem. Phys.*

(12) We are concluding an investigation of the IR spectra of alkali perchlorates using  $^{18}\text{O}$  substitution and  $^{35}\text{Cl}/^{37}\text{Cl}$  isotopic shifts. So far, the available reports on alkali perchlorates are those by G. Ritzhaupt and J. P. Devlin, *J. Chem. Phys.*, **62**, 1982 (1975), and J. Draeger, G. Ritzhaupt, and J. P. Devlin, *Inorg. Chem.*, **18**, 1808 (1979).

(13) K. Nakamoto in "Infrared and Raman Spectra of Inorganic and Coordination Compounds", Wiley, New York, 1978, pp 142-146.

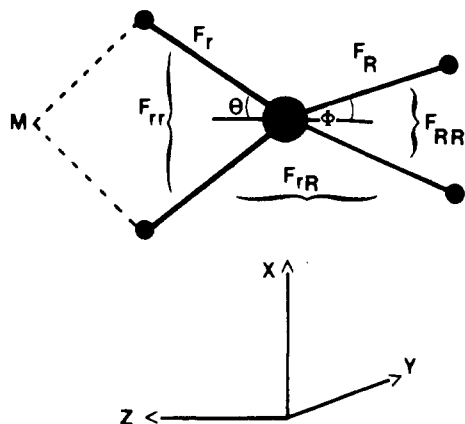


Figure 3. Vibrational model adopted for a  $C_{2v}$   $MReO_4$  molecule.

structural conclusion on  $^{18}O$ -enrichment experiments. Random  $^{18}O$  substitution in  $C_{2v}$  symmetry  $TlReO_4$  produces nine isotopomers: four of  $C_{2v}$  symmetry ( $TlRe^{16}O_4$ ,  $TlRe^{18}O_4$ , and two mixed  $TlRe^{16}O_2^{18}O_2$  species), one of  $C_1$  symmetry ( $TlRe^{16}O_2^{18}O_2$ ), and four of  $C_s$  symmetry (two different  $TlRe^{16}O_3^{18}O$  and  $TlRe^{16}O^{18}O_3$  species). The structure of each  $TlReO_4$  isotopomer is shown in Figure 2, and their stretching modes are correlated in the various symmetries in Table II. The frequencies and the relative intensities of the IR isotopic bands can be calculated to predict the IR pattern of an  $^{18}O$ -enriched perrhenate. We shall adopt a vibrational model that only considers the stretching vibrations of the  $ReO_4^-$  anion in the  $C_{2v}$  symmetry. The basic assumption in the adopted model is that the vibrations of the  $ReO_4^-$  anion are uncoupled from the remaining fundamentals. This is a harmless approximation that predicts the isotopic IR patterns with a surprising accuracy in ionic complexes in which the high-frequency modes are practically uncoupled from the low-frequency vibrations.<sup>4,5,11</sup> In this model (see Figure 3),  $F_R$ ,  $F_r$ ,  $F_{RR}$ ,  $F_{Rr}$ , and  $F_{rr}$  are the force constants for the stretching modes of the ( $R$ ) terminal and ( $r$ ) bridged rhenium-oxygen bonds and their respective interactions. Different sets of calculated frequencies have been obtained for the modes of  $^{18}O$ -enriched  $TlReO_4$ . The availability of the experimental frequencies of  $TlRe^{16}O_4$ , of  $TlRe^{18}O_4$ , and of the mixed isotopomers made possible the use of some constraints to improve the fitting between the calculated and observed frequencies. The four force constants have been allowed to vary under the condition that the most reliable force constants are those that produce the least difference between the observed and calculated  $^{16}O/^{18}O$  isotope shifts. The additional constraint is that  $F_{RR} > F_{Rr} > F_{rr}$ . The use of 108 and 98° as terminal and bridged  $OReO$  bond angles, respectively, has been done to calculate the  $^{16}O/^{18}O$  isotopic frequencies of  $TlReO_4$ . Finally, the IR isotopic intensities could be evaluated from the well-known relationships based on the bond dipole approach<sup>14</sup>

$$\sum_K I_K \propto \sum_{ij} \frac{\partial u}{\partial S_i} \frac{\partial u}{\partial S_j} G_{ij} \quad (1)$$

$$\sum_K \frac{I_K}{\lambda_K} \propto \sum_{ij} \frac{\partial u}{\partial S_i} \frac{\partial u}{\partial S_j} F_{ij}^{-1} \quad (2)$$

This procedure has already been adopted to interpret the isotopic pattern of  $CsReO_4$ .<sup>7</sup>

Regarding the agreement between the calculated and observed frequencies, it must be noted that the results are quite satisfactory and the differences are within a few wavenumbers

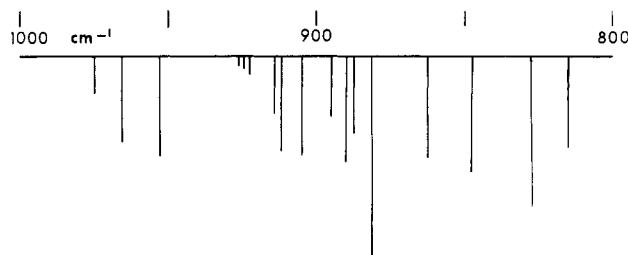


Figure 4. Line diagram relative to the IR isotopic pattern of  $^{18}O$ -enriched  $TlReO_4$  (50%  $^{18}O$  enrichment).

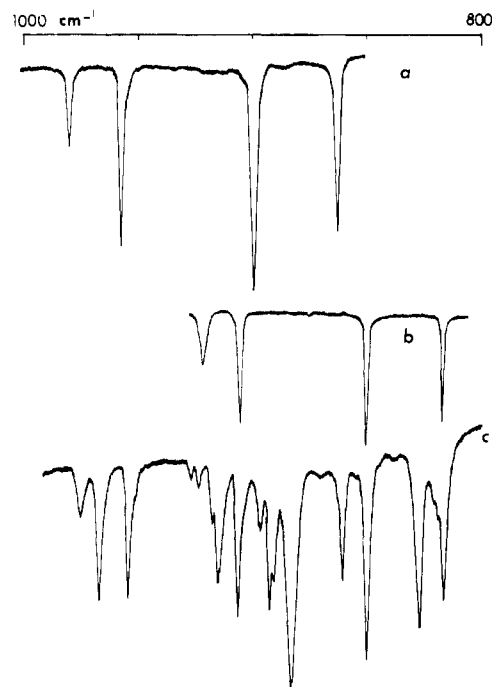


Figure 5. IR spectra ( $N_2$  matrix) of (a)  $TlReO_4$  ( $^{16}O$  natural abundance), (b)  $TlRe^{18}O_4$ , and (c)  $^{18}O$ -enriched  $TlReO_4$ .

especially for the isotopically pure  $TlRe^{18}O_4$  and the highly  $^{18}O$ -enriched isotopomers. This is mainly due to the use in the calculations of the experimentally measured rather than the zero-order frequencies and the fact that the isotope calculations have been based on the harmonic oscillator approximation and that anharmonic corrections have not been taken into account.<sup>14</sup> This introduces an oversimplification in the model, but anharmonic coefficients can hardly be obtained from the matrix spectra.

Some simplifications can be expected for the IR isotope pattern because some close lying bands might combine their intrinsic intensities into a single absorption. Not only vibrations occurring at identical frequencies but also bands spaced a few wavenumbers apart are bound to appear as peaks of reinforced intensity. The most evident predicted overlaps are for the  $B_1(a)$ ,  $A''(c)$ ,  $B_1(f)$  modes calculated at 860.3  $cm^{-1}$  and for the  $B_2(a)$ ,  $A''(b)$ ,  $B_2(d)$  modes at 952.8  $cm^{-1}$ . The other possible overlaps arising from close lying vibrations are the  $B_1(d)$ ,  $B_1(i)$ ,  $A''(g)$  modes calculated at 815.6  $cm^{-1}$ ,  $A_1(d)$ ,  $A_1(i)$ ,  $A''(g)$  at ca 849  $cm^{-1}$ ,  $A'(b)$ ,  $A(e)$ ,  $A'(h)$  at ca. 826.5  $cm^{-1}$ ,  $A'(g)$ ,  $A(e)$  at ca. 912  $cm^{-1}$ ,  $A'(h)$ ,  $A_1(i)$  at ca. 923  $cm^{-1}$ , and  $B_2(f)$ ,  $B_2(i)$ ,  $A''(h)$  at ca. 904  $cm^{-1}$ . These overlapping bands and some other ones contribute to the reinforcement of some of the fundamentals of  $TlReO_4$  and of  $CsReO_4$ ,<sup>7</sup> and it is a typical feature of these molecules. The experimental results confirm these expectations. The line diagram in Figure 4 simulates the ultimate IR isotopic pattern of  $^{18}O$ -enriched  $TlReO_4$ . The IR spectra of  $TlRe^{16}O_4$ , of  $TlRe^{18}O_4$ , and of the  $^{18}O$ -enriched sample are shown in Figure 5, and the observed

(14) E. B. Wilson, Jr., J. C. Decius, and P. C. Cross in "Molecular Vibrations—The Theory of Infrared and Raman Vibrational Spectra", Dover Publications, New York, 1980.

**Table III.** Assignments of the Isotopic Frequencies ( $\text{cm}^{-1}$ ) of  $^{18}\text{O}$ -Enriched  $\text{TlReO}_4$ 

obsd <sup>a</sup>	calcd <sup>b</sup>	assgmt <sup>c</sup>		
976.1	976.0	(a) $\text{TlRe}^{16}\text{O}_4$	$A_1$	$C_{2v}$
975.1	975.1	(b) $\text{TlRe}^{16}\text{O}_3^{18}\text{O}$	$A_1$	$C_s$
974.6	974.3	(d) $\text{TlRe}^{16}\text{O}_2^{18}\text{O}_2$	$A_1$	$C_{2v}$
966.0	966.7	(c) $\text{TlRe}^{16}\text{O}_3^{18}\text{O}$	$A_1$	$C_s$
	966.0	(e) $\text{TlRe}^{16}\text{O}_2^{18}\text{O}_2$	$A$	$C_1$
953.4	965.4	(g) $\text{TlRe}^{16}\text{O}^{18}\text{O}_3$	$A'$	$C_s$
	952.8	(a) $\text{TlRe}^{16}\text{O}_4$	$B_2$	$C_{2v}$
	952.8	(d) $\text{TlRe}^{16}\text{O}_2^{18}\text{O}_2$	$B_2$	$C_{2v}$
	952.8	(b) $\text{TlRe}^{16}\text{O}_3^{18}\text{O}$	$A'$	$C_s$
926.3	926.7	(f) $\text{TlRe}^{16}\text{O}_2^{18}\text{O}_2$	$A_1$	$C_{2v}$
922.4	924.0	(h) $\text{TlRe}^{16}\text{O}^{18}\text{O}_3$	$A'$	$C_s$
	922.0	(i) $\text{TlRe}^{18}\text{O}_4$	$A_1$	$C_{2v}$
916.2	913.7	(c) $\text{TlRe}^{16}\text{O}_3^{18}\text{O}$	$A'$	$C_s$
914.0	912.1	(e) $\text{Tl}^{16}\text{O}^{18}\text{O}_2$	$A$	$C_1$
	911.2	(g) $\text{TlRe}^{16}\text{O}^{18}\text{O}_3$	$A'$	$C_s$
905.2	903.9	(f) $\text{TlRe}^{16}\text{O}_2^{18}\text{O}_2$	$B_2$	$C_{2v}$
	903.9	(h) $\text{TlRe}^{16}\text{O}^{18}\text{O}_3$	$A'$	$C_s$
	903.9	(i) $\text{TlRe}^{18}\text{O}_4$	$B_2$	$C_{2v}$
	895.3	895.4	(a) $\text{TlRe}^{16}\text{O}_4$	$A_1$
892.0	891.3	(f) $\text{TlRe}^{16}\text{O}_2^{18}\text{O}_2$	$A_1$	$C_{2v}$
882.2	883.8	(b) $\text{TlRe}^{16}\text{O}_3^{18}\text{O}$	$A_1$	$C_s$
	883.1	(c) $\text{TlRe}^{16}\text{O}_3^{18}\text{O}$	$A'$	$C_s$
	882.8	(e) $\text{TlRe}^{16}\text{O}_2^{18}\text{O}_2$	$A$	$C_1$
	882.2	(h) $\text{TlRe}^{16}\text{O}^{18}\text{O}_3$	$A'$	$C_s$
860.1	860.3	(a) $\text{TlRe}^{16}\text{O}_4$	$B_1$	$C_{2v}$
	860.3	(f) $\text{TlRe}^{16}\text{O}_2^{18}\text{O}_2$	$B_1$	$C_{2v}$
	860.3	(c) $\text{TlRe}^{16}\text{O}_3^{18}\text{O}$	$A'$	$C_s$
	849.6	849.1	(d) $\text{TlRe}^{16}\text{O}_2^{18}\text{O}_2$	$A_1$
827.7	848.7	(i) $\text{TlRe}^{18}\text{O}_4$	$A_1$	$C_{2v}$
	848.1	(g) $\text{TlRe}^{16}\text{O}^{18}\text{O}_3$	$A'$	$C_s$
	826.6	(b) $\text{TlRe}^{16}\text{O}_3^{18}\text{O}$	$A'$	$C_s$
817.4	826.6	(e) $\text{TlRe}^{16}\text{O}_2^{18}\text{O}_2$	$A$	$C_1$
	826.5	(h) $\text{TlRe}^{16}\text{O}^{18}\text{O}_3$	$A'$	$C_s$
	815.6	(d) $\text{TlRe}^{16}\text{O}_2^{18}\text{O}_2$	$B_1$	$C_{2v}$
	815.6	(i) $\text{TlRe}^{18}\text{O}_4$	$B_1$	$C_{2v}$
	815.6	(g) $\text{TlRe}^{16}\text{O}^{18}\text{O}_3$	$A'$	$C_s$

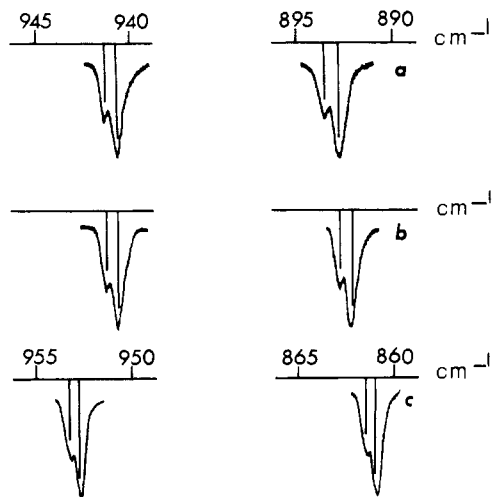
<sup>a</sup>  $\text{N}_2$  matrix spectrum. <sup>b</sup> The calculations are based on  $F_R = 8.082$ ,  $F_r = 6.750$ ,  $F_{RR} = 0.387$ ,  $F_{rr} = 0.380$ , and  $F_{Rr} = 0.383$  (mdyn/Å) and  $2\theta = 108^\circ$  and  $2\phi = 98^\circ$  as the  $\text{OReO}$  terminal and bridged bonds. <sup>c</sup> The letters in parentheses stand for the corresponding isotopomers reported in Table II and shown in Figure 2.

frequencies are reported in Table III along with the vibrational assignment performed on the basis of the discussed calculations.  $^{18}\text{O}$ -enrichment experiments demonstrate for  $\text{TlReO}_4$  the  $C_{2v}$  structure already proposed for  $\text{CsReO}_4$ . Our experiments also confirm the results of a gas-phase electron diffraction study on  $\text{TlReO}_4$ .<sup>9</sup> Identical conclusions would hold for  $\text{KReO}_4$  for which an erroneous monodentate structure had been proposed.<sup>6</sup>

#### Distortion of the $\text{ReO}_4^-$ Anion in $C_{2v}$ $\text{MReO}_4$ Perrhenates

The IR matrix of the  $\text{MReO}_4$  molecules allow one to discuss the distortion of the  $\text{ReO}_4^-$  anion from the tetrahedral geometry when it is coordinated to a metal in a bidentate manner. Information on distorted-tetrahedral oxyanions can be obtained from the evaluation of the bond angles. In  $C_{2v}$  perrhenates one terminal and one bridged  $\text{OReO}$  angle is present. Reliable electron diffraction data are available for  $\text{CsReO}_4$ <sup>8</sup> and  $\text{TlReO}_4$ <sup>9</sup> while the geometrical parameters of  $\text{KReO}_4$ <sup>6</sup> require a reinvestigation because the present spectroscopic study would show that gaseous  $\text{KReO}_4$  is a  $C_{2v}$  bidentate ionic complex.

The analysis of a resolvable fine structure of some of the stretching modes of the  $\text{ReO}_4^-$  anion would allow the evaluation of the  $\text{OReO}$  bond angles. Under a resolution better than  $0.5 \text{ cm}^{-1}$ , it would be possible to measure the Re isotope shift due to the  $^{185}\text{Re}$  and  $^{187}\text{Re}$  naturally occurring isotopes. When the simplified vibrational model for the  $\text{ReO}_4^-$  anion stretching vibrations is adopted, it may be shown that the  $\text{OReO}$  terminal

**Figure 6.** Fine structure of the  $B_2$  and  $B_1$  modes observed in the IR spectra ( $\text{N}_2$  matrix) of (a)  $\text{RbReO}_4$ , (b)  $\text{CsReO}_4$ , and (c)  $\text{TlReO}_4$ .**Table IV.** Fine Structure of the  $B_1$  and  $B_2$   $\text{ReO}_4^-$  Stretching Modes<sup>a</sup>

	$\text{RbReO}_4$		$\text{CsReO}_4$		$\text{TlReO}_4$		
	obsd <sup>b</sup>	calcd	obsd <sup>b</sup>	calcd	obsd <sup>b</sup>	calcd	
$B_1$	$^{185}\text{Re}-^{16}\text{O}$	893.6	893.6	892.8	892.9	861.4	861.4
	$^{187}\text{Re}-^{16}\text{O}$	893.1	893.1	892.3	892.4	861.0	861.0
$B_2$	$^{185}\text{Re}-^{16}\text{O}$	941.4	941.4	941.1	941.0	953.3	953.3
	$^{187}\text{Re}-^{16}\text{O}$	940.9	940.9	940.6	940.5	952.7	952.8

	$\text{RbReO}_4$	$\text{CsReO}_4$	$\text{TlReO}_4$
$2\theta$ (terminal) <sup>c</sup>	109	109.5	108
$2\phi$ (bridged) <sup>c</sup>	102	103	98
$F_{B_1}$ <sup>d</sup>	6.812	6.795	6.367
$F_{B_2}$ <sup>d</sup>	7.492	7.523	7.695

<sup>a</sup> The observed and calculated frequencies are in  $\text{cm}^{-1}$ . <sup>b</sup> Observed in  $\text{N}_2$  matrix. <sup>c</sup> Units are in deg. <sup>d</sup> Units are mdyn/Å.

bond angle ( $2\theta$ ) and the  $\text{OReO}$  bridged angle ( $2\phi$ ) can be evaluated from eq 3 and 4, respectively. In these equations,

$$\sin^2 \theta = \frac{M_x M_x^i [(\omega_{B_2}^i)^2 - (\omega_{B_2})^2]}{2M_O [M_x (\omega_{B_2})^2 - M_x^i (\omega_{B_2}^i)^2]} \quad (3)$$

$$\sin^2 \phi = \frac{M_x M_x^i [(\omega_{B_1})^2 - (\omega_{B_1}^i)^2]}{2M_O [M_x (\omega_{B_1})^2 - M_x^i (\omega_{B_1}^i)^2]} \quad (4)$$

$M_x$ ,  $M_x^i$ , and  $M_O$  are the atomic masses of  $^{185}\text{Re}$ ,  $^{187}\text{Re}$ , and  $^{16}\text{O}$ , respectively, and  $\omega$  and  $\omega_i$  the zero-order  $B_2$  and  $B_1$  frequencies of the  $^{185}\text{Re}^{16}\text{O}$  and  $^{187}\text{Re}^{16}\text{O}$  stretching modes. The calculations performed on  $\text{CsReO}_4$  and  $\text{TlReO}_4$  indicate that the  $^{185}\text{Re}/^{187}\text{Re}$  isotopic shifts on the  $B_2$  and  $B_1$  modes is ca.  $0.5 \text{ cm}^{-1}$ . The  $\text{N}_2$  matrix spectra of all the perrhenates have been examined at a resolution of ca.  $0.3 \text{ cm}^{-1}$ . The  $B_2$  and  $B_1$  bands of  $\text{RbReO}_4$ ,  $\text{CsReO}_4$ , and  $\text{TlReO}_4$  show a fine structure, while no convincing fine structure seems to be present in the spectra of the other perrhenates. Naturally occurring rhenium is a mixture of the  $^{185}\text{Re}$  and  $^{187}\text{Re}$  isotopes with abundances of 37.5% and 62.5%, respectively. The fine structure of the  $B_2$  and  $B_1$  modes observed in the IR  $\text{N}_2$  matrix spectra of  $\text{RbReO}_4$ ,  $\text{CsReO}_4$ , and  $\text{TlReO}_4$  is shown in Figure 6. The line diagrams accompanying the observed high resolution contours of the  $B_2$  and  $B_1$  bands would suggest that this fine structure arises from the rhenium isotopic shift.

The use of the observed rhenium isotopic frequencies in eq 3 and 4 allows the evaluation of the bond angles in the respective  $\text{MReO}_4$  species. The results of these calculations are reported in Table IV, and it is worth noticing that the bond

angles of matrix-isolated  $\text{CsReO}_4$  and  $\text{TlReO}_4$  are practically identical with the electron diffraction values.<sup>8,9</sup> Although the bond angles of the other perrhenates cannot be evaluated since no fine structure could be resolved, they are not expected to be very different from those of Rb and Cs perrhenates.

The amount of splitting of the  $\nu_3(\text{T}_2)$  mode of the "free"  $\text{ReO}_4^-$  anion also gives some indications of the distortion in the  $\text{C}_{2v}$ -coordinated  $\text{MReO}_4$  species. The  $\text{B}_2$  and  $\text{B}_1$  components of the splitting are separated by ca.  $51 \text{ cm}^{-1}$  in  $\text{LiReO}_4$ , ca.  $58 \text{ cm}^{-1}$  in the other alkali-metal perrhenates, and ca.  $93 \text{ cm}^{-1}$  in  $\text{TlReO}_4$ . These splittings have been measured in a  $\text{N}_2$  matrix. All the perrhenates follow the same trend in an Ar matrix, although the splittings are higher ( $87.5, 70, 60, 61.3, 60.3,$  and  $111.8 \text{ cm}^{-1}$  in the  $(\text{Li} \rightarrow \text{Tl})$  range. These splittings are not very large, especially those measured in  $\text{N}_2$  matrix.

It is evident that the coordinated  $\text{ReO}_4^-$  anion is slightly distorted from the tetrahedral geometry in all the  $\text{MReO}_4$  molecules.  $\text{TlReO}_4$  and probably  $\text{LiReO}_4$  are among the perrhenates in which the anion is more distorted.

The use of the bond moment additivity approximation<sup>14</sup> on the adopted vibrational model is a useful approach that satisfactorily predicts some relationships between relative IR band intensities. For the  $\text{A}_1, \text{B}_2$  and  $\text{B}_1$  intensity bands related to the corresponding stretching modes of the  $\text{ReO}_4^-$  anion, the following relationships can be written

$$\frac{\sum I(\text{A}_1)}{I(\text{B}_2)} = \frac{G_{11} \cos^2 \phi - 2G_{12} \cos \phi \cos \theta + G_{22} \cos^2 \theta}{G_{44} \sin^2 \theta}$$

$$\frac{\sum I(\text{A}_1)}{I(\text{B}_1)} = \frac{G_{11} \cos^2 \phi - 2G_{12} \cos \phi \cos \theta + G_{22} \cos^2 \theta}{G_{33} \sin^2 \phi}$$

$$\frac{I(\text{B}_2)}{I(\text{B}_1)} = \frac{G_{44} \sin^2 \theta}{G_{33} \sin^2 \phi}$$

where

$$G_{11} = \frac{M_{\text{Re}} + 2M_{\text{O}} \cos^2 \phi}{M_{\text{O}}M_{\text{Re}}}$$

$$G_{12} = \frac{2}{M_{\text{Re}}} (1 - 2 \sin^2 \xi)$$

$$G_{22} = \frac{M_{\text{Re}} + 2M_{\text{O}} \cos^2 \theta}{M_{\text{O}}M_{\text{Re}}}$$

$$G_{33} = G(\text{B}_1) = \frac{M_{\text{Re}} + 2M_{\text{O}} \sin^2 \phi}{M_{\text{O}}M_{\text{Re}}}$$

$$G_{44} = G(\text{B}_2) = \frac{M_{\text{Re}} + 2M_{\text{O}} \sin^2 \theta}{M_{\text{O}}M_{\text{Re}}}$$

and  $M_{\text{O}}$  and  $M_{\text{Re}}$  stand for the atomic mass of oxygen and of rhenium, respectively, and  $\xi$  is the half of the angle between the  $\text{MO}_2\text{Re}$  and  $\text{ReO}_2$  planes. These ratios lead to interesting conclusions about the distortion of the  $\text{ReO}_4^-$  anion in the coordinated  $\text{MReO}_4$  molecules. First of all, the two  $\text{A}_1$  modes cannot be separately considered in this treatment because they are coupled with each other through the  $G_{12}$  element of the  $\text{A}_1$ -symmetrized block of the G matrix. Furthermore, the relative IR band ratios depend on  $\theta$  and  $\phi$  (the angle  $\xi$  is automatically determined when  $\theta$  and  $\phi$  have been fixed), which are the half-values of the  $\text{OREO}$  terminal and bridged angles, respectively. It may be shown that for  $2\theta = 2\phi = 109^\circ 28'$  (tetrahedral angle value) the  $I(\text{B}_2):I(\text{A}_1):I(\text{B}_1)$  ratios are practically 1:1:1. Therefore, in case of no geometrical distortion, the  $\nu_3(\text{T}_2)$  mode equally distributes its intensity to each component of the triplet. The intensity of the IR-activated  $\nu_1(\text{A}_1)$  mode is very low and completely negligible with respect

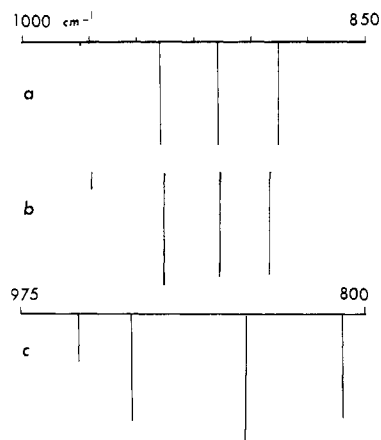


**Figure 7.** Calculated IR band intensity patterns of the stretching modes of the  $\text{ReO}_4^-$  anion: (a)  $\text{MeReO}_4$  species,  $2\theta = 2\phi = 109^\circ 28'$ ; (b)  $\text{CsReO}_4$ ,  $2\theta = 109^\circ 30'$  and  $2\phi = 103^\circ$  (see ref 2); (c)  $\text{TlReO}_4$ ,  $2\theta = 108^\circ$  and  $2\phi = 98^\circ$  (see ref 9).

to the intensity of the  $\text{A}_1$  partner. Any distortion of the  $\text{ReO}_4^-$  anion will alter the intensity ratios among the IR bands because  $2\theta$  and  $2\phi$  assume different values. In particular, the  $\text{A}_1$  modes are likely to gain intensity at the expense of the  $\text{B}_2$  and  $\text{B}_1$  modes. The effect of the distortion of the  $\text{ReO}_4^-$  anion on the intensity of the IR bands can be followed by inspection of Figure 7. The first line diagram simulates the IR spectrum of the stretching modes of a  $\text{ReO}_4^-$  anion in which the coordination leaves all the  $\text{OREO}$  bond angles tetrahedral. The splitting components are bands of identical intensity; the higher  $\text{A}_1$  mode must also be present, but its intensity is very low in the scale used so that it cannot be observed. The line diagrams in Figure 7b,c have been calculated for  $\text{CsReO}_4$  and  $\text{TlReO}_4$  by using the respective electron diffraction bond angles. The IR intensity pattern of  $\text{CsReO}_4$  is not much different from that of an undistorted perrhenate. The distortion is present in the case of  $\text{TlReO}_4$ , and this is evident in its IR spectrum from the enhancement of the intensity of the  $\text{A}_1$  modes, which is remarkable for the higher frequency  $\text{A}_1$  vibration.

The IR spectra of all the alkali perrhenates have similar intensity patterns, and this indicates that the  $\text{ReO}_4^-$  anion is not largely distorted from the tetrahedral geometry. We are currently extending our matrix-isolation studies to a range of gaseous  $\text{MXO}_4$  molecules such as alkali  $\text{MClO}_4$ ,  $\text{BaMoO}_4$ ,  $\text{BaWO}_4$ , and  $\text{EuWO}_4$ . We anticipate that these molecules are isostructural with the  $\text{MReO}_4$  molecules. In particular the IR matrix spectra of the barium and europium systems mirror the IR intensity pattern of  $\text{TlReO}_4$ . The  $\text{MoO}_4^{2-}$  and  $\text{WO}_4^{2-}$  anions are likely to be considerably distorted from the tetrahedral bond angle. The computed IR intensity pattern of  $\text{BaWO}_4$ , for example, can be fitted with the experimentally measured intensities if the bridged  $\text{OWO}$  angle is ca.  $83^\circ$ .  $^{18}\text{O}$ -substitution experiments are planned to unequivocally assign the IR spectra of these high-temperature molecules.

#### Dimerization of the $\text{MReO}_4$ Species

The results of mass spectrometric investigations indicate that the predominant species in the vapors of the alkali and thallium perrhenates is the monomer. Rubidium,<sup>15</sup> cesium,<sup>16</sup> and thallium<sup>17</sup> perrhenates are almost exclusively present in the vapor phase as  $\text{MReO}_4$  monomers; for these perrhenates the concentration of gaseous dimers is so negligible that it does not produce a detectable IR signal. The percentage of dimers is comparatively higher in  $\text{LiReO}_4$ ,<sup>18</sup>  $\text{NaReO}_4$ ,<sup>19</sup> and  $\text{KReO}_4$ .<sup>19</sup>

(15) K. Skudlarski and W. Lukas, *J. Less-Common Met.*, **31**, 329 (1973).

(16) K. Skudlarski, *Rocz. Chem.* **47**, 1611 (1973).

(17) W. Lukas and K. Skudlarski, *Rocz. Chem.* **48**, 593 (1974).

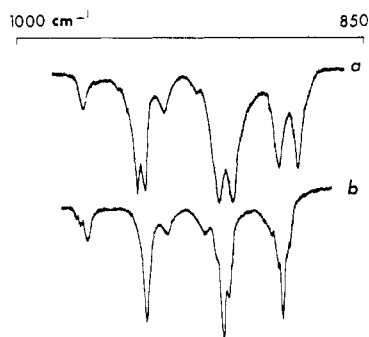


**Figure 8.** IR spectra (Ar matrix at 13 K after annealing at 35 K) of (a) NaReO<sub>4</sub> and (b) KReO<sub>4</sub>.

However, the matrix spectra of these perrhenates do not show the presence of dimers. It is well-known that matrix-isolation spectroscopy experiments are usually carried out in vaporization conditions that are quite different from those employed in mass spectrometry. Monomeric MReO<sub>4</sub> perrhenates are the only species that have been matrix isolated in the adopted conditions reported in the Experimental Section. Additional bands can be, however, observed when the matrices are warmed at the typical diffusion temperatures or when the effusing vapors are matrix isolated at 25 K or from rapid spray-on depositions. These additional features can be assigned to (MReO<sub>4</sub>)<sub>x</sub> aggregates. An argon matrix appears likely to favor the polymerization of the MReO<sub>4</sub> monomers. In fact the IR spectra obtained even from very dilute Ar matrices at 13 K show a certain complexity that is not present in the N<sub>2</sub> matrices. Several experiments employing different conditions have been carried out to gain a convincing picture on the possible polymers.

M<sub>2</sub>(ReO<sub>4</sub>)<sub>2</sub> dimers are the most likely aggregates that are produced by warming the matrices up to ca. 40 K; beyond this temperature the diffusion cannot be controlled and clusters become the predominant species. Further, we can assess that the stretching vibrations of the ReO<sub>4</sub><sup>-</sup> anion in the dimer M<sub>2</sub>(ReO<sub>4</sub>)<sub>2</sub> lie at frequencies very close to those of the monomer while the more complex aggregates are gathered around the central component of the triplet.

The IR spectra of NaReO<sub>4</sub> and KReO<sub>4</sub> isolated in Ar matrices are shown in Figure 8a,b, respectively, after annealing at 35 K. The bands present in the Ar matrix spectrum of NaReO<sub>4</sub> at 944.0, 910.3, and 884.1 cm<sup>-1</sup> (at 915.0 and 893.1 cm<sup>-1</sup> in case of KReO<sub>4</sub>) appear with an increased intensity after the annealing, which indicates that the Ar matrix favors the aggregation of the monomeric species. This fact is particularly enhanced in the Ar matrix spectra of RbReO<sub>4</sub> and TlReO<sub>4</sub>, which are reported in Figure 9a,c, respectively. The contrast between these spectra with the corresponding ones in a N<sub>2</sub> matrix is evident. These spectra have been investigated under a resolution of 0.3 cm<sup>-1</sup>. Figure 9a shows the IR Ar spectra of RbReO<sub>4</sub> under the ordinary resolution (1.0 cm<sup>-1</sup>) and Figure 9b at 0.3 cm<sup>-1</sup>. The two lower frequency doublets are resolved in the components at 910.2–906.7 cm<sup>-1</sup> and at 884.9–881.3 cm<sup>-1</sup>. These doublets have a more complex band contour, and both the upper and lower doublets also show a further component at 907.9 and 882.4 cm<sup>-1</sup>, respectively. The two higher frequency bands can be resolved into additional bands at 969.1–968.2 and 943.1–941.3 cm<sup>-1</sup>. Rhenium isotope effect cannot be claimed to explain any of the resolved bands because the observed shifts are larger than the expected ones that would range around 0.5 cm<sup>-1</sup>. Further, the intensities of these peaks do not fit with the expected IR band intensity

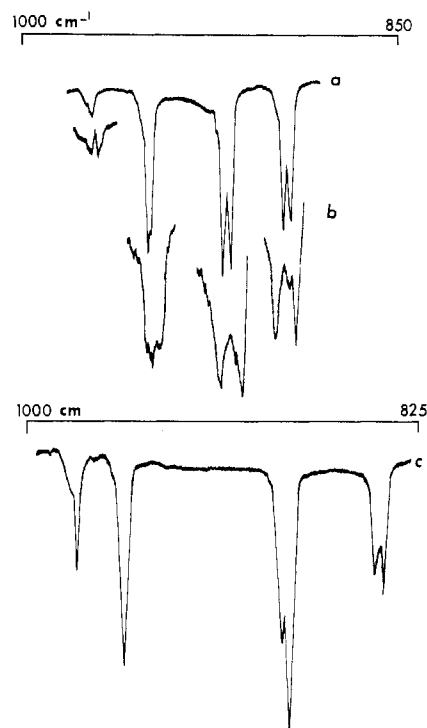


**Figure 9.** IR spectra (Ar matrix) of (a) RbReO<sub>4</sub>, (b) RbReO<sub>4</sub> at a resolution of 0.3 cm<sup>-1</sup>, and (c) TlReO<sub>4</sub>.

**Table V.** IR Frequencies (cm<sup>-1</sup>) of MReO<sub>4</sub> Dimers

	N <sub>2</sub> matrix	Ar matrix
LiReO <sub>4</sub>	951.8, ~931, 912.5, 888.3	961.8, 804.9, 871.8
NaReO <sub>4</sub>	914.1, 890.8	944.0, 910.3, 884.1
KReO <sub>4</sub>	935.2, 920.6, 903.8	915.0, 893.1
RbReO <sub>4</sub>	973.2, 944.2, 920.6, 900.0	969.1, 942.5, 910.2, 884.9
CsReO <sub>4</sub>	934.6, 920.0	909.8, 886.2
TlReO <sub>4</sub>	952.9, 900.7, 862.7	~980, 930.5, 887.0, 847.5

pattern due to the rhenium isotopes. Annealings up to 35 K do not produce appreciable effects on the intensities of the bands, and other weaker features appear; moreover, the steeply sloping background makes the picture more difficult to assess something more conclusive. It would, however, seem that in the case of RbReO<sub>4</sub> the features at 969.1, 941.1, 910.2, and 884.9 cm<sup>-1</sup> might belong to the dimer. The possible dimers of TlReO<sub>4</sub> might be identified in the bands at ~980, 930.5, 887.0, and 847.5 cm<sup>-1</sup>.

A summary of the bands assigned to the M<sub>2</sub>(ReO<sub>4</sub>)<sub>2</sub> dimers is given in Table V.

A more complete picture on the dimers is not possible with the available data. These dimers are likely to have the same structure of D<sub>2h</sub> symmetry proposed for the dimers of Cs<sub>2</sub>SO<sub>4</sub> and Cs<sub>2</sub>WO<sub>4</sub>.<sup>20</sup> The stretching modes of the ReO<sub>4</sub><sup>-</sup> anions in the D<sub>2h</sub> dimer are the 2 A<sub>g</sub> + B<sub>2g</sub> + B<sub>3g</sub> + 2 B<sub>1u</sub> + B<sub>2u</sub> + B<sub>3u</sub> vibrations. Only the "u" modes are IR active; they are the (B<sub>2u</sub> + B<sub>3u</sub>) and the (B<sub>1u</sub> + B<sub>2u</sub>) vibrations of the terminal and bridged rhenium–oxygen bonds, and the former modes would occur at higher frequencies than the latter ones. These absorptions might not be too much shifted from the monomer vibrations. The Ar matrix spectra of RbReO<sub>4</sub> and TlReO<sub>4</sub> and the broadness of the contour of the bands of the perrhenates isolated in Ar matrices would support this statement. For example, the annealed Ar spectra of RbReO<sub>4</sub> and TlReO<sub>4</sub> show a broad contour in correspondence of the highest A<sub>1</sub> mode, which under a resolution of 0.5 cm<sup>-1</sup> appears as a doublet. The highest frequency component of this doublet

(18) K. Skudlarski and W. Lukas, *J. Less-Common Met.*, **33**, 171 (1973).

(19) K. Skudlarski, J. Drowart, G. Exsteen, and A. Vander Auwera-Mahieu, *Trans. Faraday Soc.*, **63**, 1146 (1967).

(20) R. M. Atkins and K. A. Gingerich, *High Temp. Sci.*, **14**, 103 (1981).

(975.5  $\text{cm}^{-1}$  for  $\text{RbReO}_4$  and 980  $\text{cm}^{-1}$  for  $\text{TlReO}_4$ ) is observed after annealing and might belong to the dimer species. Spoliti and Stafford<sup>21</sup> have studied the gas-phase IR spectra of the alkali perrhenates. These authors have observed a broad band extending from 800 to 1000  $\text{cm}^{-1}$ . Our experiments show that the broad absorption quoted in that previous work is due to the overlap of the stretching vibrations assigned by us to the  $C_{2v}$   $\text{MReO}_4$  species. These authors have carried out extensive superheating experiments that, however, did not cause any change in frequencies or in band contours. Spoliti and Stafford came to the conclusion that the broad band observed during their experiments is due in part to the monomer and to the dimer whose frequencies are not much shifted from those of the monomer. We have also carried out superheating experiments on  $\text{LiReO}_4$ ,  $\text{NaReO}_4$ , and  $\text{KReO}_4$  whose vapor phases are supposed to consist of a nonnegligible concentration of dimers.<sup>18,19</sup> These perrhenates have been vaporized from an alumina double oven with an effusion hole of 1 mm. The

top and the base of this oven have been kept at ca. 850 and 815 K, respectively. The vapors have been collected in  $\text{N}_2$  and Ar matrices, and the observed spectra have been found identical with those obtained in the usual vaporization conditions.

We also conclude that the absorptions of the dimers might not be shifted much from those of the monomers, but they are not coincident with the bands of the  $\text{MReO}_4$  species.

**Acknowledgment.** This work has been performed under the auspices of the R. A. Welch Foundation (Grant A-387).

**Note Added in Proof.** Meanwhile, we have completed our study on the  $\text{MReO}_4$  molecules with Raman matrix-isolation measurements and with  $^{18}\text{O}$ -enrichment experiments on  $\text{KReO}_4$ .<sup>22</sup> The latter ones confirm for  $\text{KReO}_4$  the  $C_{2v}$  symmetry structure which is common for all the  $\text{MReO}_4$  monomers.

**Registry No.**  $\text{LiReO}_4$ , 13768-48-4;  $\text{NaReO}_4$ , 13472-33-8;  $\text{KReO}_4$ , 10466-65-6;  $\text{RbReO}_4$ , 13768-47-3;  $\text{CsReO}_4$ , 13768-49-5;  $\text{TlReO}_4$ , 14013-75-3;  $^{18}\text{O}$ , 14797-71-8.

(21) M. Spoliti and F. E. Stafford, *Inorg. Chim. Acta*, **2**, 301 (1968).

(22) L. Bencivenni, H. M. Nagarathna, K. A. Gingerich, and R. Teghil, *J. Chem. Phys.*, in press.

Contribution from the Department of Chemistry,  
University of Virginia, Charlottesville, Virginia 22906

## Charge-Transfer-Induced IR Absorptions in Mixed-Valence Compounds

K. Y. WONG\*

Received August 2, 1983

Prediction of the existence of tunneling transitions or charge-transfer-induced IR absorption in mixed-valence compounds has been made by Schatz et al. recently, on the basis of exact diagonalization of their PKS model. However, their claim has been disputed by Hush, who stated without proof that such transitions do not exist and are *artifacts* of the PKS model. To clarify this, the PKS model that describes a dimeric mixed-valence system is reexamined with use of linear response theory and a perturbative calculation. Both approaches give results that are consistent with Schatz et al.'s prediction. In addition, analytical expressions for the transition energies of the charge-transfer-induced IR absorption and the charge-transfer or intervalence absorptions are derived, together with expressions for their relative intensities. These are found to be in good agreement with that calculated by the numerical diagonalization method (PKS model). Applications of these expressions to some mixed-valence systems are also presented.

### 1. Introduction

Prediction of the existence of strong tunneling transitions<sup>1</sup> in the now famous Creutz-Taube ruthenium complex<sup>3</sup> is still a subject of controversy.<sup>4,5</sup> Schatz et al.<sup>1</sup> originally predicted that for this Ru complex there should be strong near-IR transitions at energies 131, 362, and 613  $\text{cm}^{-1}$  with a combined dipole strength of 0.3 D<sup>2</sup> (D = Debye). However, Krausz et al.<sup>6</sup> recently reported that such transitions are not observed experimentally. In a recent review, Wong and Schatz<sup>4</sup> suggested that, by reducing the vibronic coupling parameter in the PKS model, the calculated tunneling transition intensities could be substantially reduced and become consistent with Krausz et al.'s result, as well as with the bond-length data of the complex. However, with such a reduced value, the predicted intervalence band contour would become narrower and hence fail to fit the experimental absorption band.

This discrepancy can be removed when solvent effects are introduced into the PKS model, as shown in a recent article by Wong and Schatz.<sup>7</sup> By introduction of an "effective" solvent vibronic coupling parameter  $\lambda_s$  and assumption of an effective solvent vibrational frequency of about 200  $\text{cm}^{-1}$ , the observed absorption band shape of the Ru complex can be satisfactorily accounted for.

So far the existence of near-IR tunneling transitions is based entirely on exact numerical solution of the PKS model. In this approach, the vibronic Hamiltonian describing a dimer system is diagonalized with a large but truncated basis set. The resulting eigenfunctions are then used to calculate the transition intensities. Two types of transitions are predicted. One has transition energies  $\gg \hbar\omega_\alpha$  (intervalence transitions) and the other  $\lesssim \hbar\omega_\alpha$  (near-IR tunneling or charge-transfer-induced IR transitions), where  $\omega_\alpha$  is the molecular vibrational frequency of the  $a_{1g}$  mode of the dimer system.

It is of interest to note that the Fourier transform method of Buhks,<sup>8</sup> the Hush treatment,<sup>9-11</sup> which is entirely based on

- (1) Schatz, P. N.; Piepho, S. B.; Krausz, E. R. *Chem. Phys. Lett.* **1978**, *55*, 539-542.
- (2) Piepho, S. B.; Krausz, E. R.; Schatz, P. N. *J. Am. Chem. Soc.* **1978**, *100*, 2996-3005.
- (3) Creutz, C.; Taube, H. *J. Am. Chem. Soc.* **1969**, *91*, 3988; **1973**, *95*, 1086.
- (4) Wong, K. Y.; Schatz, P. N. *Prog. Inorg. Chem.* **1982**, *28*, 369-449.
- (5) Day, P. *Int. Rev. Phys. Chem.* **1981**, *1*, 149.
- (6) Krausz, E. R.; Burton, C.; Broomhead, J. *Inorg. Chem.* **1981**, *20*, 434.
- (7) Wong, K. Y.; Schatz, P. N. In "Mechanistic Aspects of Inorganic Reactions"; Rorabacher, D. B., Endicott, J. F., Eds.; American Chemical Society: Washington, DC, 1982; ACS Symp. Ser. No. 198, pp 281-299.
- (8) Buhks, E. Ph.D. Dissertation, Tel Aviv University, Tel Aviv, Israel, 1980.
- (9) Hush, N. S. *Prog. Inorg. Chem.* **1967**, *8*, 391-444; *Electrochim. Acta* **1968**, *13*, 1005.
- (10) Hush, N. S. "Mixed Valence Compounds"; Brown, D. B., Ed.; Reidel: Dordrecht, The Netherlands, 1980; pp 151-188.

\* Address correspondence to General Electric Co., Charlottesville, VA 22906.